Preprints of the 21st IFAC World Congress (Virtual)
Berlin, Germany, July 12-17, 2020

Formation Control with Orientation Alignment and Constrained Input

Yu-Wen Chen * **Ming-Li Chiang** ** **Li-Chen Fu** ***

* *Department of Electrical Engineering, National Taiwan University, Taipei, Taiwan, (email: r06921005@ntu.edu.tw).*
** *Graduate Institute of Automation Technology, National Taipei University of Technology, Taipei, Taiwan, (email: minglichiang@ntu.edu.tw)*
*** *Department of Electrical Engineering, and the Center for Artificial Intelligence and Advanced Robotics, National Taiwan University, Taipei, Taiwan, (e-mail: lichen@ntu.edu.tw)*

Abstract: We design a formation controller for Multi Agent Systems such that the agents can form into the desired shape and track a given reference trajectory. The main feature of the proposed design is that not only the orientation of individual agents, but also the orientation of the whole formation is considered and is designed to be aligned with the moving direction of the reference trajectory, which helps the tracking movement to be smoother compared with the common tracking results. Moreover, the control inputs are designed in predefined input ranges to reflect the practical system. System stability is proved based on nonlinear system theory and some simulations are given to validate the proposed results.

Keywords: Multi-agent systems; Nonlinear adaptive control; Coordination of multiple vehicle systems.

1. INTRODUCTION

Recently, Multi-Agent System (MAS) is extensively developed and many related topics are studied such as the consensus algorithm (Qin et al. (2011), Ni and Cheng (2010), and Meng et al. (2013)), communication topology (Li et al. (2018); Tran and Yucelen (2016); Dong and Hu (2016); Zhao (2018)), and formation control (Li et al. (2018), Zhao et al. (2018)) , etc. By the rapidly development of hardware and software, formation control of MAS possesses great opportunities in practical applications. The main target of formation control is to steer a group of agents to form into some predefined formation and to perform some desired tasks. Such control system includes system model, communication graph, information measurement property, and some additional performance requirements. We briefly discuss the related works about formation control in the following. Global or centralized communications are usually assumed in earlier works such as Leonard and Fiorelli (2001). Recently, local or distributed communications are considered in Verginis et al. (2017), Oh and Ahn (2014), Lin et al. (2014), and Sakurama (2016). Different tasks such as rotation motion (Li et al. (2018)), obstacle avoidance (Zhao et al. (2018)), constrained inputs (Yang et al. (2014), Meng et al. (2013), Zhao et al. (2018)), time-varying formation shape (Briñón-Arranz et al. (2014), Tran and Yucelen (2016)), or connectivity preservation (Verginis et al. (2017), Peng et al. (2019)), ..., etc, are related topics in the design of formation control system.

In this paper, we design a new formation controller for a MAS with numbered agents and random initial conditions such that the system will form into the desired formation shape and track a given reference trajectory. The main feature of the proposed design is that the MAS orientation is considered and is designed to be aligned with the moving direction of the reference centroid, which leads to a more "natural" tracking motion. While in the existing results, such as Yu and Liu (2016), only the orientation of individual agents are considered and the resultant tracking movement. Furthermore, the designed control inputs are constrained in some ranges, which is more practical. For the considered formation tasks, a global reference frame is usually required to obtain the descriptions of predefined desired displacement vectors used for controller design, such as Loria et al. (2014), Yu and Liu (2016), Tran and Yucelen (2016), Ge and Han (2017), Li et al. (2017), Hua et al. (2017), and Dong and Hu (2016).

In summary, the main contributions of this paper are as follows. First, we propose a formation controller that considers orientation alignment of the whole MAS in addition to that of the individual agents, and thus a more "natural" tracking motion can be achieved. Second, the controller is implemented within the constrained linear velocity and angular velocity, which is more practical in real application, and is more involved in both design and stability analysis.

This paper is organized as follows: in Section 2, we give the problem description, and introduce some preliminaries and descriptions of the desired formation. Section 3 formulates the problem mathematically and some assumptions are given. In Section 4, the considered objectives is designed with the proposed controller and we show the stability

Preprints of the 21st IFAC World Congress (Virtual)
Berlin, Germany, July 12-17, 2020

analysis. In Section 5, we provide the simulation results. The conclusion is given in Section 6.

2. PRELIMINARIES AND THE CONSIDERED PROBLEM

Algebraic Graph Theory is used for the communication topology in the MAS. We briefly give some definitions and notations in the Preliminary.

2.1 Preliminaries

A directed graph $\mathcal{G} = (V, E)$ consists of a set of nodes V and a set of directed edges E. A directed edge pointing from V_j to $V_k \in V$ is denoted as $(k, j) \in E$. The adjacency matrix $\boldsymbol{A}$ has entries a_{kj} defined to be 1 if $(k, j) \in E$ and 0 otherwise. The in-degree matrix $\boldsymbol{D}$ is a diagonal matrix with entries d_{kk} defined as the number of edges pointing toward the node-k. The Laplacian matrix $\boldsymbol{L}$ is defined as $\boldsymbol{D} - \boldsymbol{A}$. In this paper, the graph $\mathcal{G}$ represents the directed communication where nodes and edges represent the agents and the information passing directions, respectively. Define N_k as the set of nodes with edge pointing toward agent-k, *i.e.*, the neighbors that the agent-k can receive information from, and $|N_k|$ as the total number of neighbors of agent-k. The planar rotation matrix is denoted as $\boldsymbol{R}(\phi) \in R^{2\times 2}$, which rotates counterclockwise with the given angle ϕ. Let $\boldsymbol{I}_2$ be 2-by-2 identity matrix, and $\otimes$ be the Kronecker product.

2.2 The Considered Formation Problem

The objective of this paper is twofold. First, we want to design a controller with saturated input which steers the unicycle model based numbered MAS to (i) form into predefined ordered formation, (ii) keep the centroid of such desired formation tracking a given reference centroid trajectory, and (iii) align its orientation with the trajectory's direction. We give the detailed problem formulation in the following section.

3. PROBLEM FORMULATION

In this section, we first discuss the presentation of desired formation, and then give the problem formulation mathematically.

3.1 Description of the Desired Formation with Number Orders

To facilitate the realization of the controller in each agent's local frame, we propose a frame-invariant descriptions of desired numbered formation which is constructed as follows. Given any desired numbered formation with N-vertices, say Fig. 1, draw the vectors from the centroid to each agent and denote it as the center vectors $\boldsymbol{c}_k \in \mathbb{R}^2$ for $k = 1, \ldots, N$. Let d_k^* be the length of $\boldsymbol{c}_k$ and ϕ_{kj}^* be the desired relative *phase* (angle) between $\boldsymbol{c}_k$ and $\boldsymbol{c}_j$, where the term phase implies sign sensitivity, *i.e.*, $\phi_{kj}^* = -\phi_{jk}^*$. As a result, $\{d_k^*, \phi_{kj}^*\}$ can be used to describe the desired formation without considering a specific reference frame.

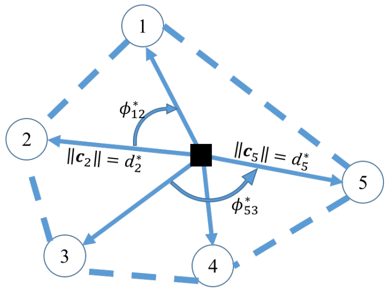

Fig. 1. The desired formation shape is given with order $1-2-3-4-5$. The centroid is labeled by the black square. The center vectors $\boldsymbol{c}_k$ with arrows have lengths d_k^*, for $k = 1, \ldots, 5$. The variable ϕ_{kj}^* is the relative angle between $\boldsymbol{c}_k$ and $\boldsymbol{c}_j$

3.2 Problem Formulation

Consider a MAS which consists of N agents with unicycle model

$$\dot{\boldsymbol{r}}_k = v_k[\cos\psi_k, \sin\psi_k]^T, \quad \dot{\psi}_k = \omega_k, \tag{1}$$

where $k = 1, 2, \ldots, N$, $\boldsymbol{r}_k \in \mathbb{R}^2$ and $\psi_k \in (-\pi, \pi]$ are agent-k's position and heading, v_k and ω_k are scalar inputs controlling linear and angular velocity, respectively. Denote the index set $\mathcal{N} = \{1, \ldots, N\}$. Given a directed communication graph $\mathcal{G}$ and the following information: **[i1]** descriptions of the desired numbered formation $\{d_k^*, \phi_{kj}^* | \forall k, j \in \mathcal{N}, k \neq j\}$, **[i2]** a smooth reference centroid trajectory $\boldsymbol{r}_0 \in \mathbb{R}^2$ which satisfies $\dot{\boldsymbol{r}}_0 = v_0[\cos\psi_0, \sin\psi_0]^T$, $\dot{\psi}_0 = \omega_0$, where v_0 and ω_0 are scalar inputs, **[i3]** the desired *constant* phase ϕ_k^* used to maintain the angle between $\boldsymbol{c}_k$ and $\dot{\boldsymbol{r}}_0$, for $k \in \mathcal{N}$, where ϕ_k^* and ϕ_j^* always satisfy $\phi_k^* - \phi_j^* = \phi_{kj}^*$, for $k, j \in \mathcal{N}$, *i.e.*, for $k \in \mathcal{N}$, we want $\boldsymbol{c}_k$ to be aligned to the direction of desired unit center vector

$$\boldsymbol{c}_k^* := [\cos(\psi_0 + \phi_k^*), \sin(\psi_0 + \phi_k^*)]^T,$$

Note that aligning $\boldsymbol{c}_k$ to $\boldsymbol{c}_k^*$ is the essential factor to achieve MAS orientation alignment. Compared with the existing results, we additionally consider tracking of ψ_0 from $\dot{\boldsymbol{r}}_0$ which leads to the more "natural" tracking motion.

As a result, we want to design the constrained control inputs v_k and ω_k with measurable information through $\mathcal{G}$ such that

$$\boldsymbol{r}_k \to \boldsymbol{r}_0 + d_k^* \boldsymbol{c}_k^* \tag{2}$$

asymptotically, for $k \in \mathcal{N}$. Here, the control inputs are constrained to specific input ranges $v_k \in [v^-, v^+]$ and $\omega_k \in [\omega^-, \omega^+]$ with predefined constants $v^-, \omega^- < 0$ and $v^+, \omega^+ > 0$. The right hand side of (2) is agent-k's desired trajectory which includes the tasks mentioned in Subsection 2.2. More precisely, d_k^* and ϕ_k^* relate to task (i), $\boldsymbol{r}_0$ relates to task (ii), $\psi_0 + \phi_k^*$ relates to task (iii). It is worth mentioning that the information given in [i2] - [i4] is "not" accessible to all agents and is obtained through the communication links. In general, only one agent will receive these exogenous information, and the rest of agents are required to estimate them. To solve the considered problem, the following assumptions are made:
(A1) The directed graph $\mathcal{G}$ is strongly connected. Moreover, at least one agent can receive the reference information, say $\boldsymbol{r}_0$, ψ_0, which is interpreted by a diagonal matrix $\boldsymbol{B}$ with entries b_{kk} be 1 if agent-k can access to reference

and 0 otherwise.

(A2) v_0, ω_0 are smooth and bounded: $v_0 \in [v_0^-, v_0^+]$ and $\omega_0 \in [\omega_0^-, \omega_0^+]$ with constants $v_0^-, \omega_0^- < 0$ and $v_0^+, \omega_0^+ > 0$. Moreover, $v_0^- > v^-, v_0^+ < v^+$ and $\omega_0^- > \omega^-, \omega_0^+ < \omega^+$, where $v^-, v^+, \omega^-, \omega^+$ are specified in [A5].

(A3) $\dot{v}_0, \dot{\omega}_0$ are bounded $\forall t \geq 0$.

(A4) $||\frac{d}{dt}(\boldsymbol{r}_0 + d_k^* \boldsymbol{c}_k^*)|| \neq 0$ for $k \in \mathcal{N}, \forall t \geq 0$. Moreover, assume that

$$v^+ > \sup_{k\in\mathcal{N},t\geq 0} [v_{max} + d_k^* \omega_{max}] := \check{v}^+$$
$$\omega^+ > \sup_{k\in\mathcal{N},t\geq 0} \mathscr{F}_k(t) := \check{\omega}^+$$
$$v^- < -\sup_{k\in\mathcal{N},t\geq 0} [v_{max} + d_k^* \omega_{max}] := \check{v}^-$$
$$\omega^- < \inf_{k\in\mathcal{N},t\geq 0} \mathscr{F}_k(t) := \check{\omega}^-$$

holds, where $v_{max} = \max(|v_0^-|, |v_0^+|)$ and $\omega_{max} = \max(|\omega_0^-|, |\omega_0^+|)$. Moreover, $\mathscr{F}_k = \frac{\ddot{\boldsymbol{r}}_k^{*T} \boldsymbol{R}(\frac{\pi}{2}) \dot{\boldsymbol{r}}_k^*}{\dot{\boldsymbol{r}}_k^{*T} \dot{\boldsymbol{r}}_k^*}$ where $\dot{\boldsymbol{r}}_k^* = \frac{d}{dt}(\boldsymbol{r}_0 + d_k^* \boldsymbol{c}_k^*)$.

Note that $\dot{\boldsymbol{r}}_k^*$ and $\mathscr{F}_k$ are agent-k's desired linear and angular velocity, respectively, where $\dot{\boldsymbol{r}}_k^*$ is from (2) and the derivation of $\mathscr{F}_k$ can be referred to Briñón-Arranz et al. (2009).

4. CONTROLLER DESIGN AND STABILITY ANALYSIS

We design the problem in three steps. In the first step, we propose an adaptive law to estimate $\boldsymbol{c}_k^*$, for $k \in \mathcal{N}$. Recall that $\boldsymbol{c}_k^*$ is considered for MAS orientation alignment task, and ψ_0 is only accessible to few agents under assumption (A1). Therefore, an adaptive estimation law is designed to estimate $\boldsymbol{c}_k^*$ via given ϕ_{kj}^*, where agent-j is the neghbor of agent-k. In the second step, we design the consensus algorithms and an observer for each agent to estimate the reference centroid velocity $\dot{\boldsymbol{r}}_0$, and the desired position errors. Here, the design of the adaptive law and the consensus algorithms are mainly inspired from the second order consensus algorithm in Ren (2007). In the third step, we derive a constrained controller to achieve (2) based on the estimations in the first and second step.

For consistence, we denote the reference information by behaviors of agent-0, and $\bar{N}_k$ as the extended set of N_k which additionally considers whether agent-k can receive information from agent-0 or not. Before proceeding to the three steps, we give the following lemma which comes form (A1) and will be used in the design:

Lemma 1. (Wen et al. (2018)). Given a directed communication graph $\mathcal{G}$ with its corresponding Laplacian matrix $\boldsymbol{L}$. Then, under assumption (A1), all eigenvalues of $\bar{\boldsymbol{L}} := \boldsymbol{L} + \boldsymbol{B}$ are positive.

4.1 Adaptive Estimation of Center Vector

Recall that $\boldsymbol{c}_k^* = [\cos(\psi_0 + \phi_k^*), \sin(\psi_0 + \phi_k^*)]^T$ stands for the MAS orientation alignment task, where $\boldsymbol{c}_k^*$ cannot be pre-given since it varies with ψ_0. Under assumption [A1], ψ_0 is not accessible to all agents, therefore, we need to estimate $\boldsymbol{c}_k$. Let $\hat{\boldsymbol{c}}_k \in \mathbb{R}^2$ be the estimation of $\boldsymbol{c}_k^*$. In the following lemma, an adaptive estimation of $\hat{\boldsymbol{c}}_k$ is proposed based on measurements through $\mathcal{G}$ and ϕ_{kj}^*.

Lemma 2. Given the communication graph $\mathcal{G}$, ψ_0, and constant ϕ_k^* for $k \in \mathcal{N}$. With assumptions [A1]-[A3], the update law

$$\begin{aligned}\dot{\hat{\boldsymbol{c}}}_k &= \hat{\boldsymbol{z}}_k \\ \dot{\hat{\boldsymbol{z}}}_k &= \frac{1}{|\bar{N}_k|} \sum_{j\in\bar{N}_k} \boldsymbol{R}(\phi_{kj}^*) \dot{\hat{\boldsymbol{z}}}_j + \frac{\alpha_1}{|\bar{N}_k|} \sum_{j\in\bar{N}_k} (\boldsymbol{R}(\phi_{kj}^*) \hat{\boldsymbol{z}}_j - \hat{\boldsymbol{z}}_k) \\ &\quad + \frac{\alpha_2}{|\bar{N}_k|} \sum_{j\in\bar{N}_k} (\boldsymbol{R}(\phi_{kj}^*) \hat{\boldsymbol{c}}_j - \hat{\boldsymbol{c}}_k) \end{aligned} \tag{3}$$

will drive $\hat{\boldsymbol{c}}_k \to \boldsymbol{c}_k^*$ exponentially, for $k \in \mathcal{N}$, where $\alpha_i > 0, i = 1, 2$. Here, $\phi_{k0}^* = \phi_k^*$, $\hat{\boldsymbol{c}}_0 = [\cos\psi_0, \sin\psi_0]^T$, $\hat{\boldsymbol{z}}_0 = \dot{\hat{\boldsymbol{c}}}_0$, $\dot{\hat{\boldsymbol{z}}}_0 = \ddot{\hat{\boldsymbol{c}}}_0$, stand for the behavior of reference trajectory from agent-0.

Proof. Let $\boldsymbol{p}_k = \boldsymbol{R}(-\phi_k^*) \hat{\boldsymbol{c}}_k$, $\boldsymbol{q}_k = \boldsymbol{R}(-\phi_k^*) \dot{\hat{\boldsymbol{c}}}_k$, and $\boldsymbol{p}_0 = \hat{\boldsymbol{c}}_0$. Pre-multiply $\boldsymbol{R}(-\phi_k^*)$ to both sides of (3), then (3) becomes

$$\begin{aligned}\dot{\boldsymbol{p}}_k &= \boldsymbol{q}_k \\ \dot{\boldsymbol{q}}_k &= \frac{1}{|\bar{N}_k|} \sum_{j\in\bar{N}_k} [\dot{\boldsymbol{q}}_j + \alpha_1(\boldsymbol{q}_j - \boldsymbol{q}_k) + \alpha_2(\boldsymbol{p}_j - \boldsymbol{p}_k)] . \end{aligned} \tag{4}$$

Based on (4), the remaining proof follows the procedures in the proof of Theorem 3.3, Ren (2007). Define $\bar{\boldsymbol{p}} = [\bar{\boldsymbol{p}}_1^T, \ldots, \bar{\boldsymbol{p}}_N^T]^T \in \mathbb{R}^{2N}$ where $\bar{\boldsymbol{p}}_k = \boldsymbol{p}_k - \boldsymbol{p}_0$, and $\tilde{\boldsymbol{p}} = (\bar{\boldsymbol{L}} \otimes \boldsymbol{I}_2)\bar{\boldsymbol{p}} \in \mathbb{R}^{2N}$. Then, (4) is equivalent to $\ddot{\tilde{\boldsymbol{p}}} + \alpha_1 \dot{\tilde{\boldsymbol{p}}} + \alpha_2 \tilde{\boldsymbol{p}} = \boldsymbol{0}$. By $\alpha_i > 0, i = 1, 2$ and Hurwitz property, $\tilde{\boldsymbol{p}}$ exponentially converges to $\boldsymbol{0}$. Moreover, $\bar{\boldsymbol{L}}$ is invertible from Lemma 1 which leads to $\bar{\boldsymbol{p}} \to \boldsymbol{0}$ exponentially. As a result, $\hat{\boldsymbol{c}}_k \to \boldsymbol{c}_k^* = [\cos(\psi_0 + \phi_k^*), \sin(\psi_0 + \phi_k^*)]^T$ exponentially.

4.2 Consensus Algorithm

By (A1), v_0 and ψ_0 are only accessible to a few agents, therefore, $\hat{v}_k$, and $\hat{\psi}_k$, $k = 1, \ldots, N$, are introduced to estimate v_0, and ψ_0, respectively. Moreover, consider (2) and let the desired position error

$$\boldsymbol{e}_k = (\boldsymbol{r}_0 + d_k^* \boldsymbol{c}_k^*) - \boldsymbol{r}_k \tag{5}$$

for $k \in \mathcal{N}$, where $\boldsymbol{r}_0$ and ψ_0 are only accessible to some agents. In this case, $\hat{\boldsymbol{e}}_k$ is introduced to estimate $\boldsymbol{e}_k$ by an observer. The consensus algorithms and the observer are derived in the following lemma.

Lemma 3. Given the graph $\mathcal{G}$, the descriptions of desired numbered formation $\{d_k^*, \phi_{kj}^*\}$, the reference centroid trajectory $\boldsymbol{r}_0$ and its velocity $\dot{\boldsymbol{r}}_0$. With assumptions (A1)-(A3), the following estimation laws

$$\dot{\hat{v}}_k = \frac{1}{|\bar{N}_k|} \sum_{j\in\bar{N}_k} \dot{\hat{v}}_j + \frac{\beta_1}{|\bar{N}_k|} \sum_{j\in\bar{N}_k} (\hat{v}_j - \hat{v}_k) \tag{6}$$

$$\dot{\hat{\psi}}_k = \frac{1}{|\bar{N}_k|} \sum_{j\in\bar{N}_k} \dot{\hat{\psi}}_j + \frac{\beta_2}{|\bar{N}_k|} \sum_{j\in\bar{N}_k} (\hat{\psi}_j - \hat{\psi}_k) \tag{7}$$

$$\begin{aligned}\dot{\hat{\boldsymbol{e}}}_k &= \beta_3 \sum_{j\in\bar{N}_k} [\hat{\boldsymbol{e}}_j - \hat{\boldsymbol{e}}_k + \boldsymbol{r}_j - \boldsymbol{r}_k + d_k^* \hat{\boldsymbol{c}}_k - d_j^* \hat{\boldsymbol{c}}_j] \\ &\quad + \hat{v}_k \boldsymbol{u}(\hat{\psi}_k) - v_k \boldsymbol{u}(\psi_k) + d_k^* \dot{\hat{\boldsymbol{c}}}_k + d_k^* \hat{\boldsymbol{c}}_k \end{aligned} \tag{8}$$

will drive $\hat{v}_k \to v_0$, $\hat{\psi}_k \to \psi_0$, $\dot{\hat{\psi}}_k \to \omega_0$, and $\hat{\boldsymbol{e}}_k \to \boldsymbol{e}_k$, exponentially, for $k \in \mathcal{N}$. Here, we define $\boldsymbol{u}(\psi) = [\cos\psi, \sin\psi]^T$, $\beta_i > 0, i = 1, 2, 3$, are design constants. Moreover, $\dot{\hat{v}}_0$, $\hat{v}_0$, $\dot{\hat{\psi}}_0$, $\hat{\psi}_0$, $\hat{\boldsymbol{e}}_0$, d_0^* are equal to

$\dot{v}_0, v_0, \dot{\psi}_0, \psi_0, [0,0]^T, 0$, respectively. Note that the index 0 represents the reference.

Proof. To prove that $\tilde{\boldsymbol{v}} \to \mathbf{0}$, $\hat{\psi}_k \to \psi_0$, we once again follow the proof of Theorem 3.3 in Ren (2007). Define $\bar{\boldsymbol{v}} = [\bar{v}_1, \ldots, \bar{v}_N]^T \in \mathbb{R}^N$ where $\bar{v}_k = \hat{v}_k - v_0$, and $\tilde{\boldsymbol{v}} = \bar{\boldsymbol{L}}\bar{\boldsymbol{v}} \in \mathbb{R}^N$. Then, (6) is equivalent to $\dot{\bar{\boldsymbol{v}}} + \beta_1 \tilde{\boldsymbol{v}} = \mathbf{0}$ with $\beta_1 > 0$ which implies $\tilde{\boldsymbol{v}} \to \mathbf{0}$ exponentially. Moreover, Lemma 1 states that $\bar{\boldsymbol{L}}$ is invertible which leads to $\bar{\boldsymbol{v}} \to \mathbf{0}$ exponentially. Similarly, (7) proves that $\hat{\psi}_k \to \psi_0$ exponentially.

Based on Lemma 2 and (8), we can prove $\hat{\boldsymbol{e}}_k \to \boldsymbol{e}_k$ exponentially. Define $\boldsymbol{\epsilon} = [\boldsymbol{\epsilon}_1^T, \ldots, \boldsymbol{\epsilon}_N^T]^T \in \mathbb{R}^{2N}$ where $\boldsymbol{\epsilon}_k = \hat{\boldsymbol{e}}_k - \boldsymbol{e}_k - d_k^*(\hat{\boldsymbol{c}}_k - \boldsymbol{c}_k^*) \in \mathbb{R}^2$, and $\boldsymbol{\delta} = [\boldsymbol{\delta}_1^T, \ldots, \boldsymbol{\delta}_N^T]^T \in \mathbb{R}^{2N}$ where $\boldsymbol{\delta}_k = \hat{v}_k \boldsymbol{u}(\hat{\psi}_k) - v_0 \boldsymbol{u}(\psi_0) \in \mathbb{R}^2$. Then, we have

$$\dot{\boldsymbol{\epsilon}} = -\beta_3(\bar{\boldsymbol{L}} \otimes \boldsymbol{I}_2)\boldsymbol{\epsilon} + \boldsymbol{\delta}. \tag{9}$$

Note that $||\boldsymbol{\delta}_k|| = ||(\hat{v}_k - v_0)\boldsymbol{u}(\hat{\psi}_k) - v_0(\boldsymbol{u}(\psi_0) - \boldsymbol{u}(\hat{\psi}_k))|| \leq ||\hat{v}_k - v_0|| + |v_0| ||\boldsymbol{u}(\psi_0) - \boldsymbol{u}(\hat{\psi}_k)||$, and by (A2) and Lipschitz continuous of $\sin(\cdot)$ and $\cos(\cdot)$, $||\boldsymbol{\delta}_k|| \leq ||\hat{v}_k - v_0|| + \sqrt{2}v^+ ||\hat{\psi}_k - \psi_0||$. As a result, $\boldsymbol{\delta} \to 0$ exponentially. Moreover, from Lemma 1, all eigenvalues of $\bar{\boldsymbol{L}} \otimes \boldsymbol{I}_2$ are positive. Thus, $\hat{\boldsymbol{e}}_k \to \boldsymbol{e}_k$ exponentially.

4.3 Constrained Control Input and Stability Analysis

The last step is to design the control laws v_k, ω_k such that $\hat{\boldsymbol{e}}_k \to \mathbf{0}$ for $k \in \mathcal{N}$. Then, with the aid of $\hat{\boldsymbol{e}}_k \to \boldsymbol{e}_k$ in Lemma 3, $\boldsymbol{e}_k \to 0$ is achieved. A design method is by second order dynamics equation, $\ddot{\hat{\boldsymbol{e}}}_k + a_1 \dot{\hat{\boldsymbol{e}}}_k + a_2 \hat{\boldsymbol{e}}_k = \mathbf{0}$ with $a_1, a_2 > 0$, as in Briñón-Arranz et al. (2014). The feasibility is guaranteed since the error equation can be rearranged into $\dot{v}_k \boldsymbol{u}(\psi_k) + \omega_k v_k \boldsymbol{R}(\frac{\pi}{2})\boldsymbol{u}(\psi_k) = \boldsymbol{f}(\cdot)$, where $\boldsymbol{f}(\cdot)$ is not a function of $\dot{v}_k$ and ω_k. Thus, $\dot{v}_k$ and ω_k are designed as $\boldsymbol{f}^T\boldsymbol{u}$ and $\frac{1}{v_k}\boldsymbol{f}^T(\boldsymbol{R}\boldsymbol{u})$, respectively. However, in such design, v_k may be close to 0 which makes ω_k large, namely, saturation is not addressed in such design. As a result, a coordination transformation is applied in this paper and thus the saturation of v_k and ω_k can be directly dealt with. To facilitate the design, we first describe agent-k's desired velocity in unicycle form.

By Lemma 2 and 3, $\hat{v}_k \boldsymbol{u}(\hat{\psi}_k) + d_k^* \dot{\hat{\boldsymbol{c}}}_k$ exponentially converges to $v_0 \boldsymbol{u}(\psi_0) + d_k^* \dot{\boldsymbol{c}}_k^*$, which is agent-$k$'s desired velocity and is equal to the derivative of the right hand side of (2). Hence, let $\check{v}_k[\cos\check{\psi}_k, \sin\check{\psi}_k]^T$, $\dot{\check{\psi}}_k (= \check{\omega}_k)$, and $\check{v}_k^*[\cos\check{\psi}_k^*, \sin\check{\psi}_k^*]^T$, $\dot{\check{\psi}}_k^* (= \check{\omega}_k^*)$ be the unicycle form of $\hat{v}_k \boldsymbol{u}(\hat{\psi}_k) + d_k^* \dot{\hat{\boldsymbol{c}}}_k$ and $v_0 \boldsymbol{u}(\psi_0) + d_k^* \dot{\boldsymbol{c}}_k^*$, respectively. Note that, $\check{v}_k$ and $\check{\omega}_k$ are the accessible estimated desired velocity for agent-k which will exponentially converge to the desired $\check{v}_k^*$ and $\check{\omega}_k^*$, respectively.

With the unicycle form of agents' desired velocities, we can derive the transformation as follows. Define $[\tilde{x}_k, \tilde{y}_k]^T := \boldsymbol{R}(-\psi_k)\hat{\boldsymbol{e}}_k \in \mathbb{R}^2$ as the transformed desired position error with respect to agent-k's moving direction, and $\tilde{\psi}_k := \check{\psi}_k - \psi_k \in \mathbb{R}$ as agent-k's heading error. Then, the error dynamics of $[\tilde{x}_k, \tilde{y}_k, \tilde{\psi}_k]^T$ is derived with (8) as

$$\begin{bmatrix} \dot{\tilde{x}}_k \\ \dot{\tilde{y}}_k \\ \dot{\tilde{\psi}}_k \end{bmatrix} = \begin{bmatrix} \omega_k \tilde{y}_k + \check{v}_k \cos\tilde{\psi}_k - v_k \\ -\omega_k \tilde{x}_k + \check{v}_k \sin\tilde{\psi}_k \\ \check{\omega}_k - \omega_k \end{bmatrix} + \begin{bmatrix} g_k^x \\ g_k^y \\ 0 \end{bmatrix}, \tag{10}$$

where $[g_k^x, g_k^y]^T = \beta_3 \boldsymbol{R}(-\psi_k) \sum_{j \in \bar{N}_k} (\hat{\boldsymbol{e}}_j - \hat{\boldsymbol{e}}_k + \boldsymbol{r}_j - \boldsymbol{r}_k + d_k^* \hat{\boldsymbol{c}}_k - d_j^* \hat{\boldsymbol{c}}_j) \in \mathbb{R}^2$, for $k \in \mathcal{N}$. As shorthands, the first and second part in the right hand side of (10) are denoted as $\boldsymbol{f}_k(\cdot)$ and $\boldsymbol{g}_k(\cdot)$, respectively. In the following, we first consider $\boldsymbol{g}_k(\cdot)$ as a perturbation and design v_k and ω_k in (10) with $\boldsymbol{g}_k(\cdot) \equiv \mathbf{0}$. Then, we prove that $\boldsymbol{g}_k(\cdot)$ asymptotically converges. Note that the perturbation term contains state information. To show the convergence of (10), a supporting lemma is stated as follows.

Lemma 4. Consider (10). Suppose (i) the unforced system, *i.e.*, when $\boldsymbol{g}_k(\cdot) \equiv \mathbf{0}$, is GAS in χ, (ii) $\boldsymbol{g}_k(\cdot)$ globally asymptotically converges to $\mathbf{0}$ in χ, and (iii) the solution of (10) is bounded. Then, the system (10) is GAS in χ, where $\chi = \{(\tilde{x}_k, \tilde{y}_k, \tilde{\psi}_k) | \tilde{x}_k \in \mathbb{R}, \tilde{y}_k \in \mathbb{R}, \tilde{\psi}_k \in (-\pi, \pi]\}$.

Proof. This lemma can be obtained from the main theorem in Sontag (1989).

The main result is shown as follows.

Theorem 5. Given the communication graph $\mathcal{G}$, the descriptions of desired numbered formation $\{d_k^*, \phi_{kj}^*\}$, the reference centroid trajectory $\boldsymbol{r}_0$ with its velocity $\dot{\boldsymbol{r}}_0$, the desired relative phase ϕ_k^* between $\boldsymbol{c}_k$ and $\dot{\boldsymbol{r}}_0$ for $k \in \mathcal{N}$. If assumptions (A1)-(A4) are satisfied, then by the control laws designed above and the constrained control law

$$\omega_k = sat_{\mathcal{W}}(\check{\omega}_k) + \frac{sat_{\mathcal{V}}(\check{v}_k)\tilde{y}_k(2 - \cos\tilde{\psi}_k)}{\gamma_1 + \frac{1}{2}\tilde{x}_k^2 + \frac{1}{2}\tilde{y}_k^2} + sat_{\vartheta}(\gamma_2 \sin\tilde{\psi}_k)$$

$$v_k = sat_{\mathcal{V}}(\check{v}_k)\cos\tilde{\psi}_k + sat_{\mathcal{X}}(\gamma_3 \tilde{x}_k), \tag{11}$$

the control objective (2) is achieved. Here $sat_{\mathcal{I}}(c)$ is a saturation function which projects scalar c into the saturated interval $\mathcal{I}$, and $\mathcal{W} = [\check{\omega}^-, \check{\omega}^+]$, $\mathcal{V} = [\check{v}^-, \check{v}^+]$, $\mathcal{X} = [-v_{gap}, v_{gap}]$ where $v_{gap} = \min(\check{v}^- - v^-, v^+ - \check{v}^+)$. Besides, γ_2, γ_3 are arbitrary positive constants, while interval ϑ and positive constant γ_1 are design parameters to ensure $\omega_k \in [\omega^-, \omega^+]$.

Proof. The considered space χ is defined as in Lemma 4. Rewrite (10) and add a small perturbation $\tilde{\boldsymbol{\Delta}}_k$ with bounded $\dot{\tilde{\boldsymbol{\Delta}}}_k$ in finite time period, we have

$$\begin{bmatrix} \dot{\tilde{x}}_k \\ \dot{\tilde{y}}_k \\ \dot{\tilde{\psi}}_k \end{bmatrix} = \begin{bmatrix} \omega_k \tilde{y}_k + sat_{\mathcal{V}}(\check{v}_k)\cos\tilde{\psi}_k - v_k \\ -\omega_k \tilde{x}_k + sat_{\mathcal{V}}(\check{v}_k)\sin\tilde{\psi}_k \\ sat_{\mathcal{W}}(\check{\omega}_k) - \omega_k \end{bmatrix} + \begin{bmatrix} g_k^x \\ g_k^y \\ 0 \end{bmatrix} + \begin{bmatrix} [\check{v}_k - sat_{\mathcal{V}}(\check{v}_k)]\cos\tilde{\psi}_k \\ [\check{v}_k - sat_{\mathcal{V}}(\check{v}_k)]\sin\tilde{\psi}_k \\ \check{\omega}_k - sat_{\mathcal{W}}(\check{\omega}_k) \end{bmatrix} + \tilde{\boldsymbol{\Delta}}_k. \tag{12}$$

Consider the right hand side of (12), where the first term is viewed as the unforced system with the rest three being perturbed inputs and denoted as $\boldsymbol{g}_k(\cdot)$, $\boldsymbol{s}_k(\cdot)$, and $\tilde{\boldsymbol{\Delta}}_k(\cdot)$, respectively. In the following, the proof is given in three steps. We first show the unforced system is GAS with (11). Then, we prove the asymptotically convergences of the three perturbed inputs. Third, we prove the boundedness of (12). Lastly, Lemma 4 is applied to prove the GAS of (12).

Consider the unforced system of (12), *i.e.*, $\boldsymbol{g}_k(\cdot) = \boldsymbol{s}_k(\cdot) = \tilde{\boldsymbol{\Delta}}_k(\cdot) \equiv \mathbf{0}$, and a Lyapunov function candidate V_k as follows:

$$V_k = \frac{1}{2}(\tilde{x}_k^2 + \tilde{y}_k^2) + (\gamma_1 + \frac{1}{2}\tilde{x}_k^2 + \frac{1}{2}\tilde{y}_k^2)(1 - \cos\tilde{\psi}_k). \tag{13}$$

Derive the time derivative of V_k, and we have

$$\begin{aligned}\dot{V}_k &= \left[sat_{\mathcal{V}}(\check{v}_k)\cos\tilde{\psi}_k - v_k\right] a_k\tilde{x}_k \\ &\quad + b_k\sin\tilde{\psi}_k\left[sat_{\mathcal{W}}(\check{\omega}_k) - \omega_k + \frac{sat_{\mathcal{V}}(\check{v}_k)a_k\tilde{y}_k}{b_k}\right] \\ &= -a_k\tilde{x}_k sat_{\mathcal{X}}(\gamma_3\tilde{x}_k) - b_k\sin\tilde{\psi}_k sat_{\vartheta}(\gamma_2\sin\tilde{\psi}_k), \quad (14)\end{aligned}$$

where $a_k = 2 - \cos\tilde{\psi}_k > 0, b_k = (\gamma_1 + \frac{1}{2}\tilde{x}_k^2 + \frac{1}{2}\tilde{y}_k^2) > 0$. Suppose the interval $\mathcal{I}$ ranges from a negative number to a positive number, then $c\,sat_{\mathcal{I}}(c) \geq 0$ and $c\,sat_{\mathcal{I}}(c) = 0$ if and only if $c = 0$. Moreover, $sat_{\mathcal{I}}(c)$ is uniformly continuous by definition. Thus, V_k is lower bounded, $\dot{V}_k \leq 0$, and $\dot{V}_k$ is uniformly continuous. As a result, by Lyapunov theorem and Invariance principle, $\dot{V}_k \to 0$ is guaranteed, which implies $\tilde{x}_k \to 0$ and $\tilde{\psi}_k \to 0$. Since $\tilde{x}_k \to 0$ means the limit exists, once again we consider the uniformly continuity of $\dot{\tilde{x}}_k$. Then, by Barbalat's lemma, $\dot{\tilde{x}}_k \to 0$ and thus $\tilde{y}_k \to 0$. Therefore, the unforced system is proved to be GAS in χ.

The next step is to show that the three perturbed inputs $\boldsymbol{g}_k$, $\boldsymbol{s}_k$, and $\tilde{\boldsymbol{\Delta}}_k$, which come from estimation error, saturation error, and singularity error, respectively, will converge to $\mathbf{0}$. For $\boldsymbol{g}_k$, consider its magnitude

$$\begin{aligned}||\boldsymbol{g}_k|| &= \beta_3||\sum_{j\in\bar{N}_k}(\hat{\boldsymbol{e}}_j - \hat{\boldsymbol{e}}_k + \boldsymbol{r}_j - \boldsymbol{r}_k + d_k^*\hat{\boldsymbol{c}}_k - d_j^*\hat{\boldsymbol{c}}_j)|| \\ &= \beta_3||\sum_{j\in\bar{N}_k}(\boldsymbol{\epsilon}_j - \boldsymbol{\epsilon}_k)||, \quad (15)\end{aligned}$$

where $\boldsymbol{\epsilon}_k$ has been proved to be exponentially converged to $\mathbf{0}$ by (9). Thus, $||\boldsymbol{g}_k|| \to 0$ exponentially. For $\boldsymbol{s}_k$, consider its magnitude, $||\boldsymbol{s}_k|| = ||[\check{v}_k - sat_{\mathcal{V}}(\check{v}_k), \check{\omega}_k - sat_{\mathcal{W}}(\check{\omega}_k)]^T||$. Thus, $||\boldsymbol{s}_k|| \leq ||[\check{v}_k - \check{v}_k^*, \check{\omega}_k - \check{\omega}_k^*]^T||$ since $\check{v}_k^* \in \mathcal{V}$ and $\check{\omega}_k^* \in \mathcal{W}$. By lemma 2 and 3, $\hat{v}_k\boldsymbol{u}(\hat{\psi}_k) + d_k^*\dot{\hat{\boldsymbol{c}}}_k \to v_0\boldsymbol{u}(\psi_0) + d_k^*\dot{\boldsymbol{c}}_k^*$ exponentially, or equivalently, $\check{v}_k \to \check{v}_k^*$ and $\check{\omega}_k \to \check{\omega}_k^*$ exponentially. Thus, $||\boldsymbol{s}_k|| \to 0$ exponentially. For $\tilde{\boldsymbol{\Delta}}_k$, it exists within finite time period, *i.e.*, $\tilde{\boldsymbol{\Delta}}_k \equiv \mathbf{0}\ \forall t \geq T$, where the relation between $\tilde{\boldsymbol{\Delta}}_k$ and $\boldsymbol{\Delta}_k$ is that $\tilde{\boldsymbol{\Delta}}_k = \left[[\boldsymbol{R}(-\psi_k)\boldsymbol{\Delta}_k]^T, 0\right]^T$.

The final step is to show the boundedness of trajectory in (12). Consider the Lyapunov candidate function (13) and derive its time derivative along the whole system (12), then we have

$$\begin{aligned}\dot{V}_k &= -a_k\tilde{x}_k sat_{\mathcal{X}}(\gamma_3\tilde{x}_k) - b_k\sin\tilde{\psi}_k sat_{\vartheta}(\gamma_2\sin\tilde{\psi}_k) \\ &\quad + \nabla V_k{}^T(\boldsymbol{g}_k + \boldsymbol{s}_k + \tilde{\boldsymbol{\Delta}}_k), \quad (16)\end{aligned}$$

where $\nabla V_k = [a_k\tilde{x}_k, a_k\tilde{y}_k, b_k\sin\tilde{\psi}_k]^T$ with loose bound:

$$\begin{aligned}||\nabla V_k|| &\leq \sqrt{9(\tilde{x}_k^2 + \tilde{y}_k^2) + \left(\gamma_1 + \frac{1}{2}\tilde{x}_k^2 + \frac{1}{2}\tilde{y}_k^2\right)^2} \\ &\leq \sqrt{\frac{9}{\tilde{x}_k^2 + \tilde{y}_k^2} + \left(\frac{\gamma_1}{\tilde{x}_k^2 + \tilde{y}_k^2} + \frac{1}{2}\right)^2}\, V_k \quad (17)\end{aligned}$$

Thus, $||\nabla V_k|| \leq c_1$ if $\tilde{x}_k^2 + \tilde{y}_k^2 \leq \mu$ and $||\nabla V_k|| \leq c_2 V_k$ if $\tilde{x}_k^2 + \tilde{y}_k^2 >= \mu$ for some positive constants c_1, c_2, μ. As a result, $||\nabla V_k|| \leq c_2V_k + c_1$ is derived. Then, by (16), we have $\dot{V}_k \leq (c_2V_k + c_1)||\boldsymbol{g}_k + \boldsymbol{s}_k + \tilde{\boldsymbol{\Delta}}_k||$. Rearrange and integrate both side from 0 to t as follows:

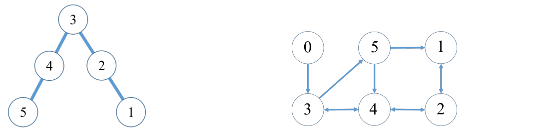

(a) Desired formation shape (b) Communication links

Fig. 2. The desired shape and the communication graph.

$$\begin{aligned}\int_0^t \frac{\dot{V}_k}{c_2V_k + c_1}\,d\tau &\leq \int_0^t ||\boldsymbol{g}_k + \boldsymbol{s}_k + \tilde{\boldsymbol{\Delta}}_k||\,d\tau \\ \frac{1}{c_2}\left[\ln(c_2V_k + c_1)\right]_0^t &\leq \int_0^\infty ||\boldsymbol{g}_k + \boldsymbol{s}_k + \tilde{\boldsymbol{\Delta}}_k||\,d\tau \quad (18)\end{aligned}$$

Recall that $||\boldsymbol{g}_k|| \to 0$, $||\boldsymbol{s}_k|| \to 0$ exponentially and $||\tilde{\boldsymbol{\Delta}}_k|| \to 0$ in finite time with small $\tilde{\boldsymbol{\Delta}}_k$ and bounded derivative when $t < T$. Thus, all of them are integrable, *i.e.*, $\int_0^\infty ||\boldsymbol{g}_k + \boldsymbol{s}_k + \tilde{\boldsymbol{\Delta}}_k||\,d\tau = c_3 < \infty$. By (18),

$$V_k(t) \leq \frac{[c_2V_k(0) + c_1]e^{c_2c_3} - c_1}{c_2} \quad (19)$$

and this proves the boundedness of (12).

By the above three steps and Lemma 4, (12) is GAS in χ and hence $\hat{\boldsymbol{e}}_k$ converges to $\mathbf{0}$. Moreover, by Lemma 2 and Lemma 3, $\hat{\boldsymbol{e}}_k \to \boldsymbol{e}_k$ is proved. As a result, $\boldsymbol{e}_k$ asymptotically converges to $\mathbf{0}$ for all k and this completes the proof.

5. SIMULATION RESULTS

In this section, we provide a simulation example for a MAS with 5 numbered agents. The communication graph is shown in Fig. 2b, where the index 0 refers to the reference information. Here we consider $\dot{\boldsymbol{r}}_0 = 0.5[\cos\psi_0, \sin\psi_0]^T$, $\dot{\psi}_0 = 0.01$, $\boldsymbol{r}_0(0) = [-4, -3]^T$. The agents' initial positions and headings are randomly selected. The simulation result is shown in the left hand side of Fig. 3, where the MAS forms into the desired numbered formation, keeps its centroid tracking $\boldsymbol{r}_0$, aligns the orientation to the direction of $\dot{\boldsymbol{r}}_0$ during tracking, and dynamically scales smaller to pass through the valley by $\boldsymbol{G}_0$. In comparison, here we also show the MAS movement without orientation alignment, which is the case in most of the existing works. Such situation can be regarded as a special case of our design where $\hat{\boldsymbol{c}}_0$ in (3) is a predefined constant without considering $\dot{\boldsymbol{r}}_0$, which results in fixed orientation of MAS. As we can see in Fig. 3, our proposed result performs more "natural" tracking movements.

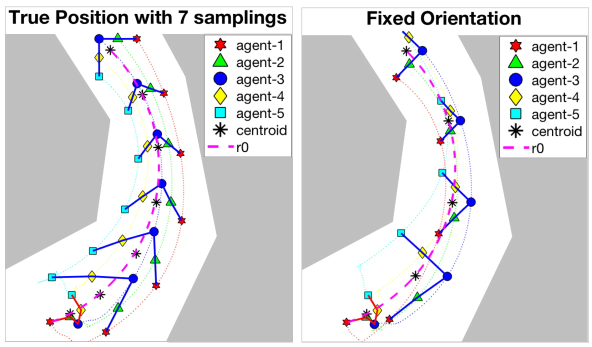

Fig. 3. (Left)MAS movement with orientation alignment and (Right)without orientation alignment.

6. CONCLUSION

In this paper, we design a new formation controller that considers MAS orientation alignment and thus the tracking motion is more natural than the results in the existing works. The numbered MAS is subject to nonholonomic constraint, and linear and angular velocity input constraints. Moreover, the proposed adaptive estimation law, consensus algorithms and constrained control inputs are shown to be stable by theory. As a result, for arbitrarily given initial conditions, the MAS forms into a desired shape whose centroid tracks the reference trajectory, and the MAS orientation is aligned with the moving direction of the reference centroid as shown in Fig. 3, which leads to a smoother movement compared with the existing works. In future work, formation control with obstacle avoidance is an interesting direction to be studied.

REFERENCES

Briñón-Arranz, L., Seuret, A., and Canudas de Wit, C. (2009). Translation control of a fleet circular formation of auvs under finite communication range. In *Proc. 48h IEEE Conf. Decision Control and 28th Chinese Control Conf.*, 8345–8350.

Briñón-Arranz, L., Seuret, A., and Canudas-de-Wit, C. (2014). Cooperative control design for time-varying formations of multi-agent systems. *IEEE Trans. Autom. Control*, 59(8), 2283–2288.

Dong, X. and Hu, G. (2016). Time-varying formation control for general linear multi-agent systems with switching directed topologies. *Automatica*, 73, 47 – 55.

Ge, X. and Han, Q. (2017). Distributed formation control of networked multi-agent systems using a dynamic event-triggered communication mechanism. *IEEE Trans. Ind. Electron.*, 64(10), 8118–8127.

Hua, Y., Dong, X., Li, Q., and Ren, Z. (2017). Distributed time-varying formation robust tracking for general linear multiagent systems with parameter uncertainties and external disturbances. *IEEE Trans. Cybern.*, 47(8), 1959–1969.

Leonard, N.E. and Fiorelli, E. (2001). Virtual leaders, artificial potentials and coordinated control of groups. In *Proc. 40th IEEE Conf. Decision Control*, volume 3, 2968–2973.

Li, S., Zhang, J., Li, X., Wang, F., Luo, X., and Guan, X. (2017). Formation control of heterogeneous discrete-time nonlinear multi-agent systems with uncertainties. *IEEE Trans. Ind. Electron.*, 64(6), 4730–4740.

Li, Y., Huang, Y., Lin, P., and Ren, W. (2018). Distributed rotating consensus of second-order multi-agent systems with nonuniform delays. *Syst. Control Lett.*, 117, 18 – 22.

Lin, Z., Wang, L., Han, Z., and Fu, M. (2014). Distributed formation control of multi-agent systems using complex laplacian. *IEEE Trans. Autom. Control*, 59(7), 1765–1777.

Loria, A., Dasdemir, J., and Jarquín-Alvarez, N. (2014). Decentralized formation-tracking control of autonomous vehicles on straight paths. In *Proc. 40th IEEE Conf. Decision Control*, 5399–5404.

Meng, Z., Zhao, Z., and Lin, Z. (2013). On global leader-following consensus of identical linear dynamic systems subject to actuator saturation. *Syst. Control Lett.*, 62(2), 132 – 142.

Ni, W. and Cheng, D. (2010). Leader-following consensus of multi-agent systems under fixed and switching topologies. *Syst. Control Lett.*, 59(3), 209 – 217.

Oh, K. and Ahn, H. (2014). Formation control and network localization via orientation alignment. *IEEE Trans. Autom. Control*, 59(2), 540–545.

Peng, Z., Wang, D., Li, T., and Han, M. (2019). Output-feedback cooperative formation maneuvering of autonomous surface vehicles with connectivity preservation and collision avoidance. *IEEE Transactions on Cybernetics*, 1–9.

Qin, J., Zheng, W.X., and Gao, H. (2011). Consensus of multiple second-order vehicles with a time-varying reference signal under directed topology. *Automatica*, 47(9), 1983–1991.

Ren, W. (2007). Multi-vehicle consensus with a time-varying reference state. *Syst. Control Lett.*, 56(7), 474 – 483.

Sakurama, K. (2016). Distributed control of networked multi-agent systems for formation with freedom of special euclidean group. In *Proc. 55th IEEE Conf. Decision Control*, 928–932.

Sontag, E.D. (1989). Remarks on stabilization and input-to-state stability. In *Proc. 28th IEEE Conf. Decision Control*, 1376–1378 vol.2.

Tran, D. and Yucelen, T. (2016). On control of multiagent formations through local interactions. In *Proc. 55th IEEE Conf. Decision Control*, 5177–5182.

Verginis, C.K., Nikou, A., and Dimarogonas, D.V. (2017). Position and orientation based formation control of multiple rigid bodies with collision avoidance and connectivity maintenance. In *Proc. 56th IEEE Conf. Decision Control*, 411–416.

Wen, G., Chen, C.L.P., and Liu, Y. (2018). Formation control with obstacle avoidance for a class of stochastic multiagent systems. *IEEE Trans. Ind. Electron.*, 65(7), 5847–5855.

Yang, T., Meng, Z., Dimarogonas, D.V., and Johansson, K.H. (2014). Global consensus for discrete-time multi-agent systems with input saturation constraints. *Automatica*, 50(2), 499 – 506.

Yu, X. and Liu, L. (2016). Distributed formation control of nonholonomic vehicles subject to velocity constraints. *IEEE Trans. Ind. Electron.*, 63(2), 1289–1298.

Zhao, S. (2018). Affine formation maneuver control of multiagent systems. *IEEE Trans. Autom. Control*, 63(12), 4140–4155.

Zhao, S., Dimarogonas, D.V., Sun, Z., and Bauso, D. (2018). A general approach to coordination control of mobile agents with motion constraints. *IEEE Trans. Autom. Control*, 63(5), 1509–1516.